School of Life Sciences[1], College of Basic Medicine[2], Lanzhou University and Key, Laboratory of Preclinical Study for New Traditional Chinese Medicine of Gansu Province[3], Lanzhou, People's Republic of China

Proanthocyanidin from grape seeds enhances anti-tumor effect of doxorubicin both *in vitro* and *in vivo*

Xiao-Yu Zhang[1, 2, 3], De-Cheng Bai[2], Yong-Jie Wu[3], Wen-Guang Li[3] and Nai-Fa Liu[1]

Received August 18, 2004, accepted September 15, 2004

Prof. Nai-Fa Liu, School of Life Sciences, Lanzhou University, Lanzhou, Gansu 730000, P.R. China
zhangxiaoyuly@yahoo.com.cn

Pharmazie 60: 533–538 (2005)

The purpose of this study was to investigate the synergistic anti-tumor effect of proanthocyanidin (PA) and doxorubicin (DOX) on K562, A549 and CNE cells *in vitro* and experimental transplantation Sarcoma 180 (S180) and Hepatoma 22 (H22) *in vivo* and to explore the mechanism of its action. PA 12.5 $\sim$ 100 mg/l inhibited proliferation of K562, A549, and CNE cells *in vitro* in a time- and concentration-dependent manner as determined by the microculture tetrazolium (MTT) assay. A combination of PA 12.5, 25 mg/l with DOX 0.01 $\sim$ 1 mg/l treatment synergistically inhibited proliferation of K562, A549, and CNE cells with decreased IC_{50} values. Under the confocal laser scanning microscope, intracellular DOX, Ca^{2+}, and Mg^{2+} concentrations were greatly increased whereas pH value and mitochondrial membrane potential were markedly reduced in K562 cells after treatment with a combination of PA plus DOX. At the same time, K562 cells showed morphological changes of apoptosis following treatment with PA plus DOX, and the administration of PA 25 mg/l plus DOX 0.3 mg/l for 24 h resulted in a significant increase in the percentage of apoptosis by flow cytometry as compared with DOX 0.3 mg/l alone ($p < 0.05$). *In vivo* experiments showed that a combination of PA 200 mg/kg i.g. with DOX 2 mg/kg i.p. treatment displayed an inhibitory effect on the growth of transplantation tumor S180 and H22 in mice compared with the DOX only group ($p < 0.01$). Taken together, these results suggest that PA enhances the DOX-induced anti-tumor effect and its mechanism is attributed to the promotion of DOX-induced apoptosis through increasing intracellular DOX, Ca^{2+} and Mg^{2+} concentrations, and reducing pH value and mitochondrial membrane potential.

1. Introduction

Proanthocyanidins are a group of naturally occurring polyphenolic bioflavonoids which are widely present in fruits, vegetables, nuts, seeds, flowers and bark, especially grape seeds. Proanthocyanidin (PA) from grape seeds has been reported to possess a wide range of biological and pharmacological activities including antibacterial, antiviral, anti-inflammatory, anti-tumor, anti-oxidative, anti-allergic and cardio-protective actions (Subarnas and Wagner 2000; Afanas'ev et al. 1989; Bagchi et al. 1997, 1998a, 1998b, 2003; Dhanalakshimi et al. 2003; Singh et al. 2004; Joshi et al. 2000; Shao et al. 2000). It has been shown to serve as one of the most potent free radical scavengers and antioxidants both *in vitro* and *in vivo* (Bagchi et al. 1997, 1998a). Our previous studies have also demonstrated that proanthocyanidin from grape seeds has an anti-inflammatory effect on experimental inflammation in rats and mice, and its mechanisms of anti-inflammatory action are relevant to oxygen free radical scavenging, anti-lipid peroxidation, and inhibition of the formation of inflammatory cytokines (Li et al. 2001).

Chemotherapeutic agents such as doxorubicin (DOX) either alone or in combination with other agents are extremely useful in the clinical treatment of cancer. One of the mechanisms of cytotoxicity of such chemotherapeutic agents is via free radical dependent mechanisms (Benner et al. 1997), and apoptosis induced by changes in intracellular ion homeostasis such as $Ca^{2+}$and Mg^{2+}, while H^+ is another mechanism (McConkey et al.1989; McConkey and Orrenius 1996; Fernandes and Cotter 1993; Simon et al. 1994). Nonetheless, chemotherapy is often associated with toxicity in normal and healthy cells and its clinical effectiveness is restricted due to dose-limiting toxic side effects including cardiotoxicity and myelotoxicity (Benner et al. 1997; Steinherz et al. 1991; Lefrak et al. 1973).

Recently, a large number of reports have demonstrated that proanthocyanidin, among other antioxidants, had an anti-tumor action and could enhance the activity of chemotherapeutic agents and diminish their toxicity to normal tissues or cells (Bagchi et al. 1999, 2001, 2002; Yamakoshi et al. 2002; Ray et al. 2000). It is generally accepted that the mechanism is partially attributable to its strong antioxidative properties. However, few studies have focused on other mechanisms of the synergistic anti-tumor effect of the combination of PA with DOX. Therefore, the aim of this study was to investigate the anti-tumor effect of PA and DOX, either alone or in combination, on K562, A549 and CNE cells *in vitro* and mice transplanta-

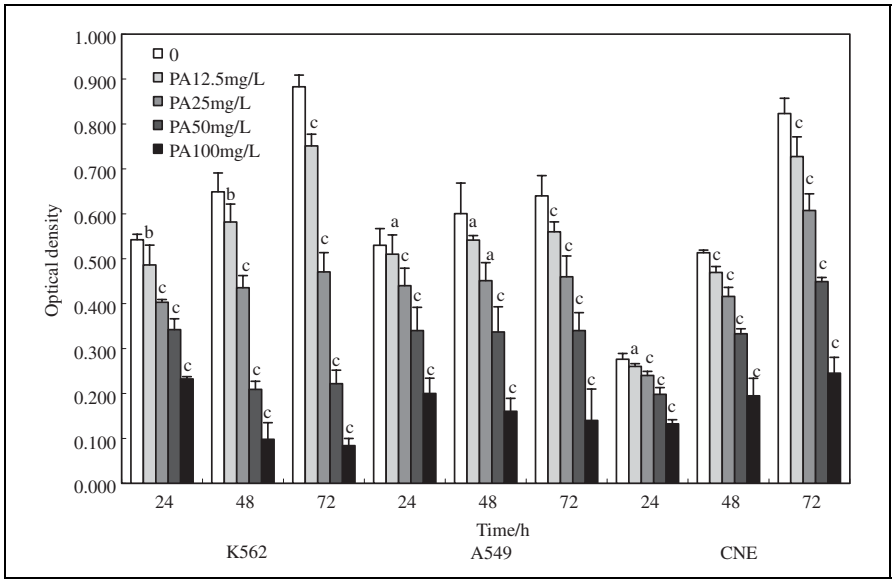

Fig. 1:
Inhibitory effects of PA 12.5 ~ 100 mg/l on K562, A549 and CNE cell proliferation *in vitro* at different times. MTT assay was used to measure cytotoxicity. Each point represents the mean ± SD of three experiments with four replicates. n = 3 experiments × 4 cultures. [a] $P > 0.05$, [b] $P < 0.05$, [c] $P < 0.01$ vs. control group

tion S180 or H22 in experimental models *in vivo*. We also explored the possible mechanism of its synergistic anti-tumor effect as judged by the significant changes in intracellular DOX accumulation, mitochondrial membrane potential and ion concentrations such as Ca^{2+}, Mg^{2+}, and H^{+}.

2. Investigations and results

2.1. Inhibitory effects on cell proliferation in vitro

In order to verify the anti-tumor effects of PA on K562, A549, and CNE cells *in vitro*, cytotoxicity was measured by the MTT assay. As shown in Fig. 1, PA 12.5, 25, 50,

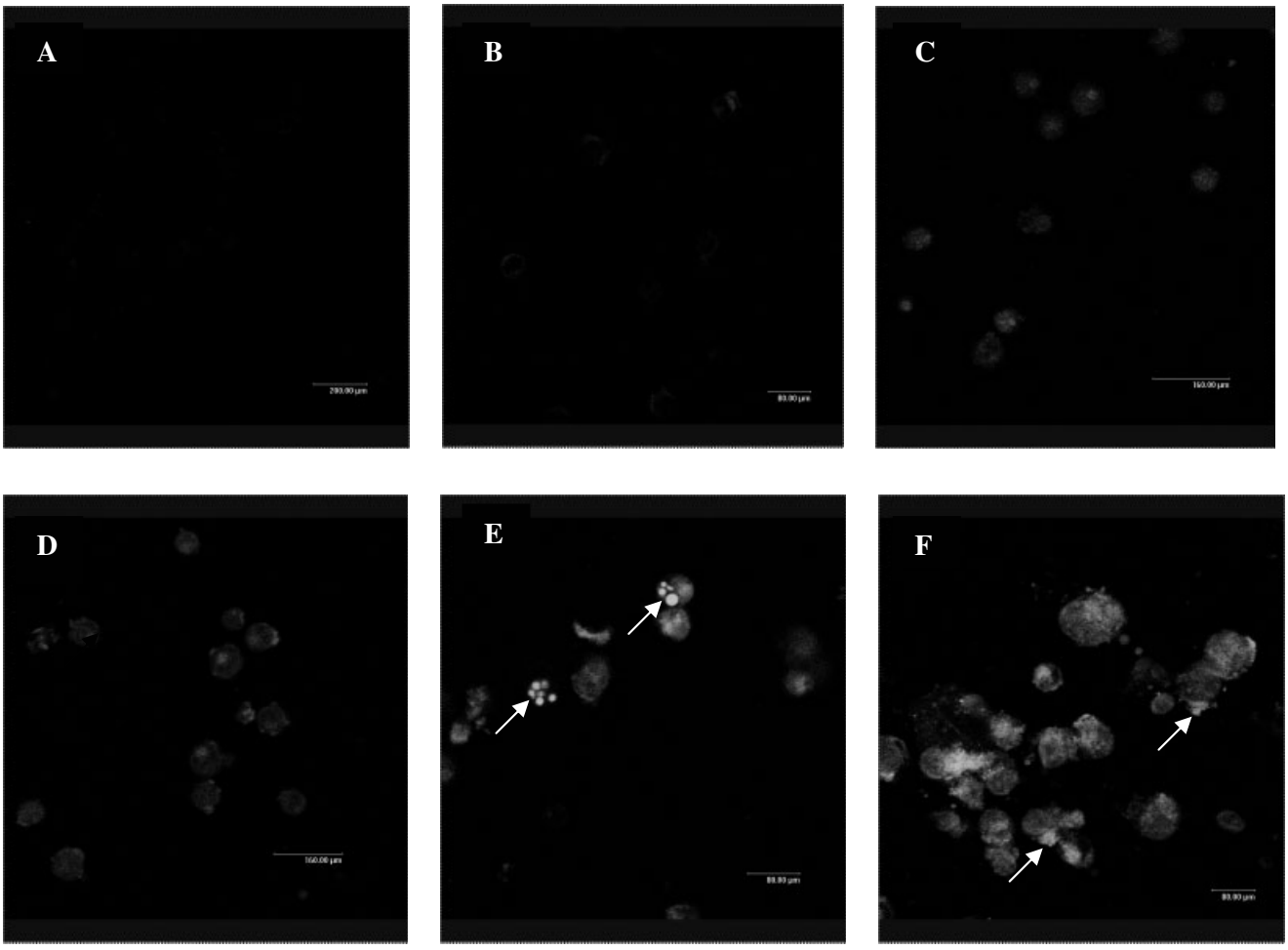

Fig. 2: Intracellular DOX accumulation and apoptotic morphological changes in K562 cells *in vitro* by confocal laser scanning microscopy after 24 h treatment. A: control; B: PA 12.5 mg/L; C: DOX 0.3 mg/L; D: DOX 0.3 mg/L + PA 12.5 mg/L; E: DOX 0.3 mg/L + PA 25 mg/L; F: DOX 0.3 mg/l + PA 50 mg/l. Intracellular fluorescence intensity of DOX accords with intracellular DOX accumulation. Apoptosis cells with powerful fluorescence bodies of nuclear fragmentation were marked by arrows

Table 1: Synergistic anti-tumor effects of PA plus DOX on K562, A549 and CNE cells *in vitro* as measured by MTT assay after 24 h administration

Concentration ($mg \cdot L^{-1}$)		K562			A549			CNE		
DOX	PA	OD_{570}	IR (%)	IC_{50} ($mg \cdot L^{-1}$)	OD_{570}	IR (%)	IC_{50} ($mg \cdot L^{-1}$)	OD_{570}	IR (%)	IC_{50} ($mg \cdot L^{-1}$)
0	0	0.336 ± 0.063		0.15	0.307 ± 0.016		0.224	0.718 ± 0.020		0.376
0.01	0	0.284 ± 0.041^{b}	15.5 ± 12.2	(0.09–0.23)	0.265 ± 0.016^{c}	13.9 ± 5.4	(0.149–0.338)	0.292 ± 0.003^{c}	4.5 ± 0.9	(0.208–0.682)
0.03	0	0.234 ± 0.030^{c}	30.2 ± 9.0		0.239 ± 0.025^{c}	22.1 ± 8.0		0.256 ± 0.009^{c}	16.4 ± 2.9	
0.1	0	0.191 ± 0.015^{c}	43.3 ± 4.4		0.181 ± 0.016^{c}	41.2 ± 5.2		0.223 ± 0.019^{c}	27.2 ± 6.2	
0.3	0	0.152 ± 0.019^{c}	54.7 ± 5.5		0.133 ± 0.013^{c}	56.6 ± 4.1		0.169 ± 0.015^{c}	44.9 ± 4.8	
1	0	0.068 ± 0.017^{c}	79.8 ± 5.1		0.104 ± 0.021^{c}	66.2 ± 6.9		0.101 ± 0.020^{c}	67.1 ± 6.4	
0.01	12.5	0.218 ± 0.017^{cfi}	35.1 ± 5.0	0.02	0.234 ± 0.019^{cei}	24.0 ± 6.1	0.074	0.270 ± 0.007^{cdg}	11.7 ± 2.3	0.136
0.03	12.5	0.141 ± 0.048^{cfi}	58.2 ± 14.2	(0.01–0.05)	0.187 ± 0.016^{cfi}	39.2 ± 5.2	(0.059–0.093)	0.215 ± 0.005^{cfi}	29.9 ± 1.8	(0.120–0.154)
0.1	12.5	0.106 ± 0.011^{cfi}	68.4 ± 3.2		0.150 ± 0.040^{cei}	51.2 ± 13.1		0.165 ± 0.017^{cfi}	46.3 ± 5.5	
0.3	12.5	0.062 ± 0.024^{cfi}	81.5 ± 7.0		0.092 ± 0.016^{cfi}	70.2 ± 5.2		0.121 ± 0.025^{cfi}	60.6 ± 8.0	
1	12.5	0.027 ± 0.019^{cdi}	92.0 ± 5.5		0.051 ± 0.028^{cfi}	83.4 ± 9.2		0.067 ± 0.012^{cei}	78.2 ± 3.8	
0.01	25	0.174 ± 0.039^{cfi}	48.2 ± 11.5	0.01	0.214 ± 0.025^{cfi}	30.3 ± 8.3	0.04	0.243 ± 0.023^{efg}	20.5 ± 7.4	0.066
0.03	25	0.126 ± 0.069^{cfi}	62.5 ± 20.6	(0.006–0.017)	0.162 ± 0.022^{cfi}	47.3 ± 7.0	(0.035–0.049)	0.188 ± 0.008^{cfi}	38.6 ± 2.8	(0.061–0.071)
0.1	25	0.075 ± 0.042^{cfi}	77.7 ± 12.4		0.117 ± 0.022^{cfi}	62.1 ± 7.0		0.131 ± 0.019^{cfi}	57.1 ± 6.3	
0.3	25	0.047 ± 0.028^{cfi}	86.0 ± 8.2		0.077 ± 0.010^{cfi}	75.1 ± 3.2		0.084 ± 0.028^{cfi}	72.7 ± 9.3	
1	25	0.008 ± 0.023^{cfi}	97.6 ± 6.8		0.030 ± 0.017	90.2 ± 5.5		0.026 ± 0.007^{cfi}	91.5 ± 2.3	
0	12.5	0.301 ± 0.006^{a}	10.3 ± 1.7	78.79	0.295 ± 0.005^{c}	4.0 ± 1.8	74.15	0.289 ± 0.006^{c}	5.7 ± 2.1	110.2
0	25	0.250 ± 0.005^{c}	25.5 ± 1.4	(54.08–114.80)	0.258 ± 0.023^{c}	16.1 ± 7.5	(43.97–125.04)	0.266 ± 0.010^{c}	13.0 ± 3.4	(40.44–300.31)
0	50	0.212 ± 0.015^{c}	36.9 ± 4.3		0.197 ± 0.030^{c}	35.8 ± 9.9		0.220 ± 0.017^{c}	28.2 ± 5.5	
0	100	0.144 ± 0.003^{c}	57.1 ± 1.0		0.118 ± 0.020^{c}	61.7 ± 6.5		0.147 ± 0.009^{c}	52.0 ± 3.1	

MTT results were expressed as the mean ± SD of three experiments with four replicates. n = 3 experiments × 4 cultures. [a] $P > 0.05$, [b] $P < 0.05$, [c] $P < 0.01$ vs control group; [d] $P > 0.05$, [e] $P < 0.05$, [f] $P < 0.01$ vs each corresponding to concentration of DOX alone; [g] $P > 0.05$, [h] $P < 0.05$, [i] $P < 0.01$ vs each corresponding to concentration of PA alone. The IC_{50} values and its 95% confidence limits (in parentheses) of DOX and PA alone or PA 12.5, 25 mg/l with DOX 0.01 ~ 1 mg/l treatment were calculated by liner regression analysis. Inhibition rate (IR %) = $(1 - OD_{570\,Treated}/OD_{570\,Control}) \times 100\%$. OD, optical density; IC_{50}, 50% growth-inhibition concentration

Table 2: Effects of DOX and PA either alone or in combination on the fluorescence intensity of intracellular DOX, Ca^{2+} and Mg^{2+} concentrations, pH value and mitochondrial membrane potential (MMP) in K562 cells after 24 h treatment

Concentration ($mg \cdot L^{-1}$)		Intracellular fluorescent intensity				
PA	DOX	DOX	Ca^{2+}	Mg^{2+}	pH	MMP
0	0	–	111.04 ± 7.63^{di}	13.24 ± 4.60^{dg}	31.56 ± 7.83^{di}	65.89 ± 2.18^{fi}
12.5	0	–	111.62 ± 4.40^{ai}	16.70 ± 4.76^{ag}	26.42 ± 5.01^{ai}	39.12 ± 5.08^{ci}
0	0.3	25.59 ± 3.85	138.48 ± 8.22^{cf}	16.42 ± 4.87^{ad}	10.28 ± 3.01^{cf}	57.79 ± 2.14^{cf}
12.5	0.3	43.81 ± 5.53^{i}	153.82 ± 4.22^{cfh}	19.17 ± 4.47^{adg}	0.70 ± 0.23^{cfi}	23.88 ± 4.71^{cfi}
25	0.3	51.50 ± 4.67^{i}	153.80 ± 5.55^{cfh}	23.49 ± 1.70^{ceh}	0.61 ± 0.28^{cfi}	22.50 ± 4.75^{cfi}
50	0.3	95.83 ± 2.45^{i}	195.49 ± 5.25^{cfi}	86.07 ± 5.85^{cfi}	0.98 ± 0.26^{cfi}	79.16 ± 2.31^{cfi}

After 24 h treatment, K562 cells were loaded with Fluo-3/AM (5 μmol/L), Mag-fluo-4 (5 mmol/L), Carboxy SNARF-1/AM (10 μmol/L), and Mito Tracker Green FM (1.25 μmol/L), respectively for 45 min at 37 °C. Additionally, DOX itself has inherent fluorescence. Thus, the fluorescence intensity changes of intracellular DOX, Ca^{2+}, Mg^{2+}, pH, and MMP in K562 cells were determined by confocal laser scanning microscopy. Results are mean ± SD of three experiments. [a] $P > 0.05$, [b] $P < 0.05$, [c] $P < 0.01$ vs control group; [d] $P > 0.05$, [e] $P < 0.05$, [f] $P < 0.01$ vs PA alone; [g] $P > 0.05$, [h] $P < 0.05$, [i] $P < 0.01$ vs DOX alone

and 100 mg/l significantly inhibited proliferation of K562, A549, and CNE cells in a time- and concentration-dependent manner. To study the synergetic anti-tumor effect of PA on K562, A549, and CNE cells treated with DOX, we combined the minimal effective concentrations 12.5, 25 mg/l of PA with DOX 0.01 $\sim$ 1 mg/l treatment. Table 1 shows that DOX 0.01 $\sim$ 1 mg/l concentration-dependently inhibited proliferation of K562, A549, and CNE cells after 24 h treatment, and the IC_{50} values were 0.15 (0.09 $\sim$ 0.23), 0.224 (0.149 $\sim$ 0.338), and 0.376 (0.208 $\sim$ 0.682) mg/l, respectively. PA 12.5, 25 mg/l enhanced DOX-induced cytotoxicity on K562, A549, and CNE cells with decreased IC_{50} values.

2.2. Intracellular DOX accumulation and apoptotic morphological changes in K562 cells

Because DOX itself has inherent fluorescence, intracellular DOX accumulation and apoptotic morphology can be observed under a confocal laser scanning microscope. The increase in fluorescence is indicative of an increase in intracellular DOX accumulation. Table 2 and Fig. 2 show the fluorescence intensity of intracellular DOX accumulation when K562 cells were treated with DOX 0.3 mg/L alone or plus PA 12.5, 25, 50 mg/l. After the combination of DOX with PA, the intracellular fluorescence intensity of DOX was dramatically increased as compared with DOX 0.3 mg/l alone ($p < 0.01$), and more apoptosis cells with powerful fluorescence bodies were observed (Fig. 2).

2.3. Effects of PA on intracellular Ca^{2+} and Mg^{2+} concentration, pH value and mitochondrial membrane potential

To investigate the mechanism of the anti-tumor effect of PA plus DOX in K562 cells, we monitored the changes of intracellular Ca^{2+} and Mg^{2+} concentration, pH value and mitochondrial membrane potential with molecular probes as detected by confocal laser scanning microscopy. As shown in Table 2, intracellular Ca^{2+} concentration was not affected after treatment with PA 12.5 mg/l alone, but it was increased with DOX 0.30 mg/l alone. The combination of DOX 0.30 mg/l and PA 12.5 $\sim$ 50 mg/l greatly increased intracellular Ca^{2+} concentration as compared with DOX alone ($P < 0.05$). Likewise, a similar effect was observed on intracellular Mg^{2+} concentration (Table 2).
However, the combination of DOX and PA markedly reduced intracellular pH value and mitochondrial membrane potential as compared with DOX alone ($p < 0.01$) (Table 2).

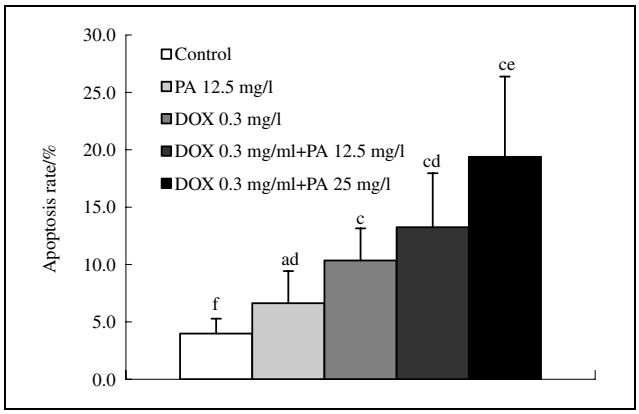

Fig. 3: Effects of PA on DOX-induced apoptosis in K562 cells *in vitro* as determined by flow cytometry. After 24 h treatment with PA and DOX alone or in combination of the two in K562 cells, apoptosis rate was calculated using Multicycle software and expressed as the number of apoptotic cells/total cells. Results are mean $\pm$ SD of three experiments. [a] $P > 0.05$, [b] $P < 0.05$, [c] $P < 0.01$ vs. control; [d] $P > 0.05$, [e] $P < 0.05$, [f] $P < 0.01$ vs. DOX alone

2.4. Effects of PA on DOX-induced apoptosis

The percentage of apoptosis was analyzed by flow cytometry after treatment with PA and DOX alone or in combination in K562 cells. As shown in Fig. 3, the apoptosis rate was increased by $10.4 \pm 2.8\%$, $13.3 \pm 4.7\%$, and $19.4 \pm 7.0\%$, respectively for DOX 0.3 mg/l alone or in combination with PA 12.5 or 25 mg/L. The administration of PA 25 mg/l plus DOX 0.3 mg/l for 24 h resulted in a significant increase in the percentage of apoptosis as compared with DOX 0.3 mg/l alone ($p < 0.05$).

2.5. Anti-tumor effects of PA in vivo

To examine the *in vivo* anti-tumor effect of PA, male Kunming mice (10 mice for each group) were inoculated subcutaneously (s.c.) into the right axillary fossa on day 0 with 3×10^6 viable tumor cells (Sarcoma 180 or Hepatoma 22) per mouse according to the protocols of transplant tumor research. Anti-tumor activity was evaluated by the percentage inhibition of tumor weight. Data reported in Table 3 show that PA 200 mg/kg intragastrically (i.g.), DOX 2 mg/kg, i.p., or PA 200 mg/kg plus DOX 2 mg/kg had a significant anti-tumor effect on the growth of S180 or H22 as compared with control ($p < 0.01$). At the same time, a combination of PA and DOX treatment markedly inhibited the tumor growth as compared with DOX alone ($p < 0.01$).

Table 3: Inhibitory effects of DOX and PA either alone or in combination on the growth of Sarcoma 180 or Hepatoma 22 in mice *in vivo*

Group	Dose ($mg \cdot kg^{-1}$)		S180		H22	
	DOX	PA	Tumor weight (g)	Inhibition rate (%)	Tumor weight (g)	Inhibition rate (%)
Control	–		2.17 ± 0.45^{f}	–	1.81 ± 0.44^{f}	–
DOX	2	0	1.12 ± 0.31^{c}	46.37 ± 15.04	0.88 ± 0.27^{c}	48.19 ± 15.77
PA	0	200	1.40 ± 0.21^{ce}	33.10 ± 10.29	1.11 ± 0.17^{cd}	34.69 ± 10.08
PA+DOX	2	200	0.68 ± 0.11^{cf}	67.44 ± 5.40	0.53 ± 0.19^{cf}	68.98 ± 11.11

On day 0 male Kunming mice were inoculated s.c. with 3×10^6 viable tumor cells (Sarcoma 180 or Hepatoma 22) each mouse in a volume of 0.2 ml. On day 1 they were treated with PA 200 mg/kg i.g. daily, doxorubicin 2 mg/kg, i.p. every other day, or PA 200 mg/kg plus doxorubicin 2 mg/kg, respectively. The mice implanted with S_{180} or H_{22} were sacrificed on day 10 and the tumors were removed and weighed. Inhibition rate (IR %) = (1 – Tumor $weight_{Treated}$/Tumor $weight_{Control}$) $\times$ 100%. Results are mean $\pm$ SD of 10 mice. [a] $P > 0.05$, [b] $P < 0.05$, [c] $P < 0.01$ vs. control; [d] $P > 0.05$, [e] $P < 0.05$, [f] $P < 0.01$ vs. DOX alone

3. Discussion

A combination of two or more anticancer compounds is ordinarily used to treat cancer patients, but it is often associated with increased toxicity to normal cells, such as those in the hematopoietic, gastrointestinal and cardiovascular systems. Consequently their doses are limited by toxicity. More recently, it has been reported that proanthocyanidin from grape seeds had an anti-tumor action without toxicity by itself, and also enhanced the effects of known anti-tumor agents and reduced their toxicity (Bagchi et al. 2001, 2002; Yamakoshi et al. 2002; Ray et al. 2000). Our results clearly demonstrated that PA significantly inhibited proliferation of K562, A549, and CNE cells in a time- and concentration-dependent manner. A combination of the minimal effective concentration 12.5, 25 mg/l of PA with DOX 0.01 $\sim$ 1 mg/l for 24 h synergistically inhibited proliferation of K562, A549, and CNE cells, and induced apoptosis of K562 cells. At the same time, *in vivo* experiments showed that a combination of PA 200 mg/kg i.g. with DOX 2 mg/kg i.p. treatment significantly inhibited the growth of S180 and H22 in mice compared with a DOX only group ($p < 0.01$). Simon et al. (1994) have established that the cytotoxicity of DOX is affected by its intracellular accumulation, which is enhanced by acidic shifts and reversed by alkaline shifts. In the present experiment, PA strongly decreased intracellular pH value and increased intracellular DOX accumulation in DOX-treated K562 cells. This suggests the possibility that the increase in intracellular DOX accumulation is associated with the reduction in intracellular pH value, which may contribute to the potentiation of the anti-tumor effect of the PA and DOX combination.

Apoptosis is not only a genetically controlled mechanism essential for the maintenance of tissue homeostasis, proper development and elimination of unwanted cells such as tumor cells (Wyllie et al. 1980), but is also a commonly-accepted mechanism of the anti-tumor effect of chemotherapeutic drugs such as DOX (Silva et al. 1996). It is presumed that perturbations in intracellular ion homeostasis could be a conspicuous manifestation of apoptosis, due to the multitude of proteins which are activated in the apoptotic cascade, and which invariably depend on the presence of certain intracellular ions (McConkey et al. 1989; McConkey and Orrenius 1996; Cotter and Fernanded 1993). Particular emphasis has been placed on the influence of Ca^{2+} ions because Ca^{2+} is one of the most important intracellular messengers. Intracellular Ca^{2+} plays a central role in the induction of apoptosis. An increase in cytosolic Ca^{2+} concentration has often been linked to the activation of a Ca^{2+}/Mg^{2+} dependent endonuclease responsible for cleavage of DNA linker regions to generate nucleosomal (180–200 base pair) fragments during the degradation phase of apoptosis cell death. More recently, the influence of Mg^{2+} ions on apoptosis has also received some attention because intracellular Mg^{2+} is the most abundant divalent metal ion in eukaryotic cells, and the role of Ca^{2+} as an intracellular messenger is incomplete without the coexistence of internal Mg^{2+} ions. Mg^{2+} is thought to be required in excess for Ca^{2+} to elicit a response. The regulatory function of Ca^{2+} is carried out in synergy with the structural function of Mg^{2+}. The Ca^{2+}/Mg^{2+} binding sites are occupied by Mg^{2+} *in vivo* to stabilize the structure of proteins, while the Ca^{2+} specific sites perform the regulatory functions. The sole contribution of Mg^{2+} to apoptosis has been thought to be its absolute requirement in the initial breakdown of DNA into large fragments of 300 and 50 kbp, prior to the dispensable event of internucleosomal cleavage (Cain et al. 1994). In this experiment, PA elevated the intracellular Ca^{2+} and Mg^{2+} concentrations of DOX-treated cells. This indicates that Mg^{2+} may be an adjunct to Ca^{2+} ions responsible for both endonuclease activity and apoptosis induction. In addition, the changes of intracellular ions such as Ca^{2+} and Mg^{2+} may induce mitochondrial apoptosis and reduce its membrane potential, and monitoring the mitochondrial membrane potential using a fluorescent technique has generally been adopted as an indicator of cell apoptosis (Nicholls and Ward 2000; Bolduc et al. 2004). We have shown that PA in the proper concentration also led to decreased mitochondrial membrane potential, which may contribute to the synergistic effect of PA on DOX-induced apoptosis.

The perturbations in intracellular ion homeostasis, pH value and mitochondrial membrane potential could be not only a conspicuous manifestation of apoptosis, but also one of the most crucial mechanisms of cytotoxicity in chemotherapeutic agents. At present, confocal laser scanning microscopy is the best means to detect intracellular ion homeostasis, DOX accumulation, pH value, and mitochondrial membrane potential. Therefore, it is concluded that the potentiation by PA of DOX-induced cytotoxicity may be attributed to the promotion of DOX-induced apoptosis through increasing intracellular DOX, Ca^{2+} and Mg^{2+} concentrations, and reducing pH value and mitochondrial membrane potential.

4. Experimental

4.1. Drugs and chemicals

Proanthocyanidin (PA), brown-red powder (purity > 96%), extracted from grape seeds and provided by the Laboratory of Applied Organic Chemistry, Lanzhou University was dissolved in 5% dimethyl sulfoxide (DMSO). Doxorubicin (DOX) was obtained from Meiji Pharmaceutical Co Ltd (Tokyo, Japan). MTT [3-(4,5-dimethylthiazol-2-yl)-2,5-diphenyl tetrazolium bromide] and sodium dodecyl sulfate (SDS) were purchased from Sigma Chemical Co (St Louis, MO, USA). RPMI-1640 medium was obtained from GIBCO BRL (Grand Island, NY, USA). Bovine serum was purchased from Hangzhou Si-Ji-Qing Biotechnology Co (Hangzhou, China). Fluo-3/AM, Mag-Fluo-4/AM, Carboxy SNARF-1/AM and Mito Tracker Green FM were purchased from Molecular Probes Inc. (Eugene, Oregon, USA). Other chemicals were of analytical purity.

4.2. Cell cultures

Human chronic myelogenous leukemia K562, human pulmonary adenocarcinoma A549 and human nasopharyngeal carcinoma CNE cells were purchased from the Cell Bank of Shanghai Institute of Cell Biology, Chinese Academy of Sciences (Shanghai, China). Cell lines were grown in complete RPMI-1640 medium containing 10% heat-inactivated bovine serum, 2 mM L-glutamine, 100 units/ml penicillin and 100 μg/ml streptomycin at 37 °C in a humidified atmosphere with 5% CO_2, and routinely passaged every other day.

4.3. MTT assay in vitro

Cytotoxicity was measured by the microculture tetrazolium (MTT) assay (Mosmann 1983). Briefly, exponentially-growing cells were washed and resuspended in complete RPMI-1640 medium to a density of 1×10^8 cells/l. 100 μl aliquots of cells containing DOX and PA alone or the two in combination were seeded in quadruplicate into 96-well flat bottom microculture plates (Costar, Corning, USA) for varying periods of time. At the end of the incubation period, MTT (5 g/l) 10 μl was added to each well and further cultured for another 4 h, then SDS 100 μl (10%, w/v, in 0.01 M HCl) was added and mixed thoroughly to dissolve formazan crystals at 37 °C. After shaking the plates for 5 min, optical density (OD) was measured at 570 nm with a Microplate Reader (ELx800 Instruments, Bio-TEK, USA). The IC_{50} values and their 95% confidence limits of DOX and PA alone or PA 12.5, 25 mg/l with DOX 0.01 $\sim$ 1 mg/l treatment were calculated by liner regression analysis (Tallarida and Murray 1981).

4.4. Observation of apoptotic morphological changes and measurement of intracellular DOX accumulation in K562 cells

Because DOX itself has inherent fluorescence, intracellular DOX accumulation and cell apoptotic morphology can be observed in K562 cells treated

with DOX 0.3 mg/L alone or plus PA 12.5, 25, 50 mg/l under a confocal laser scanning microscope (Leica TCS SP2, Leica Microsystems Heidelberg GmbH, Mannheim, Germany). Briefly, following treatment with PA and DOX, either alone or in combination, for 24 h, K562 cells were washed twice in ice-cold phosphate-buffered saline (PBS) (without Ca^{2+} and Mg^{2+}) with centrifugation. Intracellular DOX accumulation was immediately determined, and apoptotic morphological changes were simultaneously observed.

4.5. Determination of intracellular Ca^{2+} and Mg^{2+} concentration, pH value and mitochondrial membrane potential

To measure intracellular Ca^{2+} and Mg^{2+} concentration, pH value and mitochondrial membrane potential (MMP), we used Fluo-3/AM, Mag-fluo-4, Carboxy SNARF-1/AM, and Mito Tracker Green FM, respectively. After treatment as described above, K562 cells were washed twice in ice-cold PBS with centrifugation, and then loaded with Fluo-3/AM (5 μmol/l), Mag-fluo-4 (5 mmol/l), Carboxy SNARF-1/AM (10 μmol/l) or Mito Tracker Green FM (1.25 μmol/l), respectively for 45 min at 37 °C according to the manufacturer's instructions. The cells were again washed twice in PBS. The changes of intracellular Ca^{2+}, Mg^{2+}, pH value and mitochondrial membrane potential were measured by confocal laser scanning microscopy.

4.6. Apoptosis analysis by flow cytometry

Treated K562 cells as described above were washed in PBS with centrifugation, and fixed in ice-cold 70% ethanol at 4 °C for at least 24 h. The cells after fixation were washed in PBS, and stained with propidium iodide (PI) solution containing PI 50 mg/l and RNase 50 mg/l for 30 min at room temperature in the dark. The sample was read on a Coulter Epics XL flow cytometry apparatus (Beckman-Coulter Inc, Fullerton, CA, USA). The percentage of cells in the apoptotic sub-G_1 phase was calculated using Multicycle software (Phoenix Flow System, San Diego, CA, USA).

4.7. Animals and tumor transplantation in vivo

Male Kunming mice weighing 18.0–22.0 g (Grade II, Certificate No. 14-005) were purchased from the Animal Room of Lanzhou Medical College. All animal experiments were approved by the College Committee on Use and Care of Animals. According to the protocols of transplant tumor research (Wand 1997), male Kunming mice were inoculated subcutaneously (s.c.) into right axillary fossa on day 0 with 3×10^6 viable tumor cells (Sarcoma 180 or Hepatoma 22), each mouse in a volume of 0.2 ml. On day 1 the mice were randomly divided into four experimental groups ($n = 10$ mice for each group): Control, DOX, PA, and PA plus DOX groups, and treated with 0.9% normal saline i.g. daily, doxorubicin (2 mg/kg, i.p.) every other day, PA (200 mg/kg i.g.) daily, and PA 200 mg/kg plus doxorubicin 2 mg/kg, respectively. The tumor-bearing mice implanted with S180 or H22 were sacrificed on day 10 and the tumors were removed and weighed.

4.8. Statistical analysis

The *in vitro* results are expressed as mean ± SD of three separate experiments. The *in vivo* data are mean ± SD of 10 mice. Statistical comparisons were made using analysis of variance (ANOVA) followed by Student-Newman-Keuels' post hoc test for multiple comparisons with the computer statistical package (SPSS 11.0 for Window). Differences with $p < 0.05$ were considered statistically significant.

Acknowledgement: This work was supported by the Natural Science Foundation of Gansu Province, China (ZS001-A23-059-Y).

References

Afanas'ev IB, Dorozhko AI, Brodskii AV, Kostyuk VA, Potapovitch AI (1989) Chelating and free radical scavenging mechanisms of inhibitory action of rutin and quercetin in lipid peroxidation. Biochem Pharmacol 38: 1763–1769.

Bagchi D, Garg A, Krohn RL, Bagchi M, Tran MX, Stohs SJ (1997) Oxygen free radical scavenging abilities of vitamins C and E and grape seed proanthocyanidin extract *in vitro*. Res Commun Mol Pathol Pharmacol 95: 179–189.

Bagchi D, Garg A, Krohn RL, Bagchi M, Bagchi DJ, Balmoori J, Stohs SJ (1998a) Protective effects of grape seed proanthocyanidins and selected antioxidants against TPA-induced hepatic and brain lipid peroxidation and DNA fragmentation, and peritoneal macrophage activation in mice. Gen Pharmacol 30: 771–776.

Bagchi D, Kuszynski CA, Balmoori J, Bagchi M, Stohs SJ (1998b) Hydrogen peroxide-induced modulation of intracellular oxidized states in cultured macrophage J774A.1 and neuroactive PC-12 cells, and protection by a novel grape seed proanthocyanidin extract. Phytother Res 12: 568–571.

Bagchi M, Balmoori J, Bagchi D, Kuszynski CA, Stohs SJ (1999) Protective effects of vitamins C and E, and a novel grape seed proanthocyanidin extract (GSPE) on smokeless tobacco-induced oxidative stress and apoptopic cell death in human oral keratinocytes. Free Radic Biol Med 26: 992–1000.

Bagchi D, Ray SD, Patel D, Bagchi M (2001) Protection against drug- and chemical-induced multiorgan toxicity by a novel IH636 grape seed proanthocyanidin extract. Drugs Exp Clin Res 27: 3–15.

Bagchi D, Bagchi M, Stohs SJ, Ray SD, Sen CK, Preuss HG (2002) Cellular protection with proanthocyanidins derived from grape seeds. Ann New York Acad Sci 957: 260–270.

Bagchi D, Sen CK, Ray SD, Das DK, Bagchi M, Preuss HG, Vinson JA (2003) Molecular mechanisms of cardioprotection by a novel grape seed proanthocyanidin extract. Mutation Res 523–524: 87–97.

Benner E, Bishop MR, Agarwal N, Iversen P, Joshi SS (1997) Combination of antisense oligonucleotide and low-dose chemotherapy in hematological malignancies. J Pharm Toxicol Methods 37: 229–235.

Bolduc JS, Denizeau F, Jumarie C (2004) Cadmium-induced mitochondrial membrane-potential dissipation does not necessarily require cytosolic oxidative stress: studies using rhodamine-123 fluorescence unquenching. Toxicol Sci 77: 299–306.

Cain K, Inayat-Hussain SH, Kokileva L, Cohen GM (1994) DNA cleavage in rat liver nuclei activated by Mg^{2+} or $Ca^{2+} + Mg^{2+}$ is inhibited by a variety of structurally unrelated inhibitors. Biochem Cell Biol 72: 631–638.

Dhanalakshimi S, Agarwal R, Agarwal C (2003) Inhibition of NF-kappaB pathway in grape seed extract-induced apoptotic death of human prostate carcinoma DU145 cells. Int Oncol 23: 721–727.

Fernandes RS, Cotter TG (1993) Activation of a calcium magnesium independent endonuclease in human leukemic cell apoptosis. Anticancer Res 13: 1253–1259.

Joshi SS, Kuszynski CA, Bagchi M, Bagchi D (2000) Chemopreventive effects of grape seed proanthocyanidin extract on Chang liver cells. Toxicol 155: 83–90.

Lefrak EA, Pitha J, Rosenheim S, Gottlieb JA (1973) A clinicopathologic analysis of adriamycin cardiotoxicity. Cancer 32: 302–314.

Li WG, Zhang XY, Wu YJ, Tian X (2001) Anti-inflammatory effect and mechanism of proanthocyanidins from grape seeds. Acta Pharmacol Sin 22: 1117–1120.

McConkey DJ, Nicotera P, Hartzell P, Bellomo G, Wyllie AH, Orrenius S (1989) Glucocorticoids activate a suicide process in thymocytes through an elevation of cytosolic Ca^{2+} concentration. Arch Biochem Biophys 269: 365–370.

McConkey DJ, Orrenius S (1996) The role of calcium in the regulation of apoptosis. J Leukocyte Biol 59: 775–783.

Mosmann T (1983) Rapid colorimetric assay for cellular growth and survival: application to proliferation and cytotoxicity assays. J Immunol Methods 65: 55–63.

Nicholls DG, Ward MW (2000) Mitochondrial membrane potential and neuronal glutamate excitotoxicity: mortality and millivolts. Trends Neurosci 23: 166–174.

Ray SD, Patel D, Wong V, Bagchi D (2000) *In vivo* protection of DNA damage associated apoptotic and necrotic cell deaths during acetaminophen-induced nephrotoxicity, amiodarone-induced lung toxicity and doxorubicin-induced cardiotoxicity by a novel IH636 grape seed proanthocyanidin extract. Res Commun Mol Pathol Pharmacol 107: 137–166.

Shao ZH, Becker LB, Vanden Hoek TL, Schumacker PT, Li CQ, Zhao DH, Wojcik K, Anderson T, Qin YM, Dey L, Yuan CS (2003) Grape seed proanthocyanidin extract attenuates oxidant injury in cardiomyocytes. Pharmacol Res 47: 463–469.

Silva CP, Oliveira CR, Lima MCP (1996) Apoptosis as a mechanism of cell death induced by different chemotherapeutic drugs in human leukemic T-lymphocytes. Biochem Pharmacol 51: 1331–1340

Simon SM, Roy D, Schindler M (1994) Intracellular pH and the control of multidrug resistance. Proc Natl Acad Sci 91: 1128–1132.

Singh RP, Tyagi AK, Dhanalakshimi S, Agarwal R, Agarwal C (2004) Grape seed extract inhibits advanced human prostate tumor growth and angiogenesis and upregulates insulin-like growth factor binding protein-3. Int J Cancer 108: 733–740.

Steinherz LJ, Steinherz PG, Tan CC, Heller G, Murphy L (1991) Cardiac toxicity 4 to 20 years after completing anthracycline therapy. J AM Med Assoc 266: 1672–1677.

Subarnas A, Wagner H (2000) Analgesic and anti-inflammatory activity of the proanthocyanidin shellegueain A from Polypodium feei METT. Phytomedicine 7: 401–405.

Tallarida RJ, Murray RB (1981) Manual of pharmacologic calculations with computer programs. 1st ed., New York: Springer, p. 14–21.

Wand WR (1997) *In vivo* methods. In: Teicher BA (ed.) Anticancer drug development guide, preclinical screening, clinical trials, and approval. Humana Press Inc: Totowa NJ, p. 59–213.

Wyllie AH, Kerr JFR, Currie AR (1980) Cell death: the significance of apoptosis. Int Rev Cytol 68: 251–356.

Yamakoshi J, Saito M, Kataoka S, Kikuchi M (2002) Safety evaluation of proanthocyanidin-rich extract from grape seeds. Food Chem Toxicol 40: 599–607.